Scripta Materialia 203 (2021) 114089

Contents lists available at ScienceDirect

Scripta Materialia

journal homepage: www.elsevier.com/locate/scriptamat

Compression fatigue properties and damage mechanisms of a bioinspired nacre-like ceramic-polymer composite

Guoqi Tan[a,b], Qin Yu[c], Zengqian Liu[a,b,*], Xuegang Wang[a], Mingyang Zhang[a,b], Yanyan Liu[a,b], Zhefeng Zhang[a,b,*], Robert O. Ritchie[c]

[a] Shi-Changxu Innovation Center for Advanced Materials, Institute of Metal Research, Chinese Academy of Sciences, Shenyang 110016, China
[b] School of Materials Science and Engineering, University of Science and Technology of China, Hefei 230026, China
[c] Department of Materials Science and Engineering, University of California Berkeley, Berkeley, CA 94720, United States

ARTICLE INFO

Article history:
Received 25 May 2021
Revised 12 June 2021
Accepted 13 June 2021

Keywords:
Nacre-like composites
Fatigue properties
Damage mechanisms
Stress amplitude
Dental materials

ABSTRACT

Fatigue resistance is invariably critical for structural materials, but is rarely considered in the development of new bioinspired materials. Here the fatigue behavior and damage mechanisms of a nacre-like ceramic (yttria-stabilized zirconia) - polymer (polymethyl methacrylate) composite, which resembles human tooth enamel in its stiffness and hardness, were investigated under cyclic compression to simulate potential service conditions. The composite has a brick-and-mortar structure which exhibits a staircase-like fracture behavior; it displays a transition in cracking mode from the fracture of the ceramic bricks to separation along the inter-brick polymer phase with increasing stress amplitude. The nacre-like structure functions to induce crack deflection, increase the roughness of the crack surfaces, and promote the mutual sliding between bricks during fracture; this results in high fatigue resistance, which enhances the potential of this composite for dental applications.

As biological materials in nature are particularly effective in deriving outstanding mechanical efficiency from their complex structures, they are being increasingly regarded as natural prototypes for guiding the structural design of man-made materials with enhanced performance [1-4]. A notable example is the nacre in mollusk shells where aragonite platelets (~95 vol.%) are embedded within an organic matrix, forming the so-called brick-and-mortar structure. Such an architecture can facilitate a series of toughening mechanisms, *e.g.*, by plastic deformation of the organic matrix, platelet interlocking and bridging, and crack deflection along the interfaces between platelets, thereby conferring a significant increase in the fracture toughness of nacre roughly by three orders of magnitude (in energy terms), compared to that of its constituents [3,5,6]. By learning from nature, the nacre-like brick-and-mortar structure has been reproduced in a variety of man-made materials and proven to be effective in enhancing their mechanical properties [7-14]. Such an approach may even offer new opportunities for solving engineering problems. In a recent study, we fabricated a nacre-like ceramic-polymer composite composed of yttria-stabilized zirconia and polymethyl methacrylate (PMMA) [10]. By modulating the micro- to nano-scale characteristics of the brick-and-mortar structure, the Young's modulus and hardness of the composite were made essentially equal to those of the enamel in human teeth. The composite also exhibits the highest level of fracture toughness and machinability, as indicated by its lowest brittleness index (*i.e.*, the ratio of hardness to toughness) among dental materials, which can help diminish the abrasion associated with contact to antagonist teeth. Such an exceptional combination of properties makes the composite appealing for dental applications such as new tooth restorations or replacements.

Fatigue properties are critical for ensuring the durability of materials in service under cyclic loading conditions, but are often a major limitation restricting the application of new structural materials [15-17]. Specifically, for nacre-like composites, the fatigue properties have attracted far less attention than their mechanical behavior under monotonic loading conditions [7–14]. To date, only thin membranes composed of graphene, molybdenum disulfide and other nano-constituents have been probed with respect to their fatigue properties [18-21], whereas the cyclic properties of bulk-sized composites (*i.e.*, of millimeter dimensions or above) with brick-and-mortar structures have yet to be explored. Moreover, the cyclic loading in previous studies has invariably been applied parallel to the platelets or bricks in the composites [18–21]. This contradicts the scenario found for natural nacre where the cyclic loads are principally applied perpendicular to the platelets;

* Corresponding authors at: Shi-Changxu Innovation Center for Advanced Materials, Institute of Metal Research, Chinese Academy of Sciences, Shenyang 110016, China.
E-mail addresses: zengqianliu@imr.ac.cn (Z. Liu), zhfzhang@imr.ac.cn (Z. Zhang).

https://doi.org/10.1016/j.scriptamat.2021.114089
1359-6462/

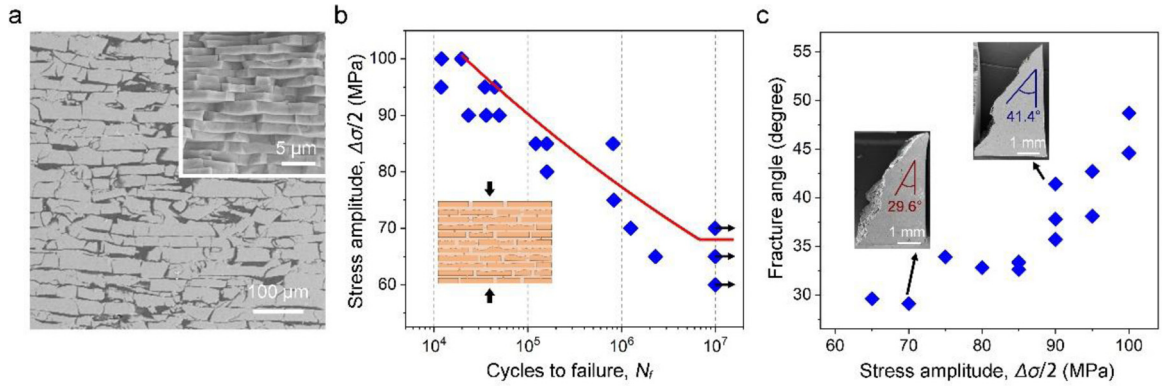

Fig. 1. Structure and fatigue properties of the bioinspired nacre-like composite. (a) The brick-and-mortar structure of the composite as compared to natural nacre (*Sinanodonta woodiana*) [5]. (b) Compression-compression fatigue stress-life data of the composite and its description using the Basquin formulation, as indicated by the red line. The loading direction for the cyclic compression is illustrated in the inset. (c) Variations in the fracture angle of the composite as a function of the applied stress amplitude $\Delta\sigma/2$. Representative appearances of the samples after fatigue fracture at relatively high and low $\Delta\sigma/2$ are shown in the insets. (For interpretation of the references to color in this figure legend, the reader is referred to the web version of this article.)

indeed, it is exactly in this loading configuration that brick-and-mortar structures can most effectively resist crack propagation so as to confer maximum resistance to fracture [3,4,7–14]. As a consequence, the fatigue properties and damage mechanisms of the nacre-like composites still remain largely unclear, especially considering the specific effects of the brick-and-mortar architecture on the fatigue cracking behavior. Clarifying such an issue would not only provide insights into the fatigue mechanisms of nacre-like composites, but may also offer guidance for the design of new fatigue-resistant materials. This is particularly important for potential dental applications of this enamel-matching composite because the human teeth, along with tooth restorations or replacements, have to withstand cyclic masticatory forces, principally in compression-compression mode, with saliva lubrication for more than 10^7 cycles throughout a typical lifespan [22–24]. Accordingly, in the present study, the fatigue properties of our nacre-like zirconia/PMMA composite were examined under cyclic compression-compression loads to be consistent with actual service conditions of human teeth. The brick-and-mortar structure was found to promote a staircase-like fracture behavior with cracking mechanisms that were dependent on the applied stress amplitude.

The nacre-like composite was fabricated by infiltrating the polymer phase into the compact of an ice-templated ceramic scaffold [10]. Specifically, the interfacial bonding between the inorganic and organic phases was strengthened by forming covalent bonds by grafting the surfaces of the scaffolds using a γ-MPS coupling agent before polymer infiltration. As noted above, the composite comprised ~77 vol.% yttria-stabilized zirconia ceramic and ~23 vol.% PMMA polymer with a brick-and-mortar structure qualitatively mimicking natural nacre, as shown in Fig. 1a. The length and thickness of the ceramic bricks were in range of 70–160 μm and 10–25 μm, respectively, giving an average aspect ratio of ~6.8. The maximum compressive strength along the direction perpendicular to the bricks and the fracture toughness for subcritical crack growth were measured to be ~265 MPa and ~9.6 MPa $m^{1/2}$, respectively. Full details on the fabrication, structure and mechanical properties (under monotonic loading conditions) of the composite can be found in Ref. [10].

The fatigue stress-life data, in terms of the number of loading cycles to failure N_f as a function of the applied stress amplitude $\Delta\sigma/2$, and its description using the Basquin formulation [17] are presented in Fig. 1b. The fatigue endurance strength of the composite, described by the critical stress amplitude to give a life exceeding 10^7 cycles, was determined to be ~68 MPa, giving a fatigue ratio, *i.e.*, the ratio of the fatigue endurance strength to the maximum compressive strength under monotonic loading condition, of ~0.26. As shown in Fig. 1c, the fracture angle of the nacre-like composite, *i.e.*, the inclination of the main fracture profile with respect to the loading axis (Fig. S1 in the Supplementary Materials), displays an increasing trend as the applied stress amplitude $\Delta\sigma/2$ increases. The small fracture angle under relatively low $\Delta\sigma/2$ is caused by the occurrence of micro-splitting in the composite, as described below. This is associated with the generation of lateral tensile stresses from local defects or stress concentrations which are principally perpendicular to the loading axis. In general, an increase in $\Delta\sigma/2$ leads to an increase in the fracture angle to around 45° where the resolved shear stress reaches the maximum on the fracture plane. This implies that the shear-induced plastic deformation may be enhanced and plays an increasing role in dominating the fatigue fracture behavior [17].

Fig. 2 shows the fatigue damage morphologies of the nacre-like composite after loading for a specific number of cycles corresponding, respectively, to the lifetime (N_f, after fracture) and half of the lifetime ($N_f/2$, without fracture) under relatively high and low stress amplitudes $\Delta\sigma/2$, *i.e.*, at 90 MPa and 65 MPa, respectively. It is seen that the composite exhibits a rough fracture surface at the microscale with crack propagation following a rather zig-zag path under relatively high $\Delta\sigma/2$, forming a series of "stairs" (Fig. 2a) [25]. The height of these "stairs" conforms roughly to the thickness of the zirconia ceramic bricks. Additionally, on the fracture surface a large number of bricks, specifically on the order of 38% of the total, are covered with a layer of polymer phase which has clearly experienced plastic deformation (Fig. 2b). This implies that the fatigue damage and crack propagation are mainly localized within the polymer phase between bricks. In comparison, the "stairs" become much less evident under relatively low $\Delta\sigma/2$ (Fig. 2c). At such low stress amplitudes, the fracture morphology indicates that the surfaces of ~75% of the ceramic bricks are clean without polymer adhesion (Fig. 2d). These bricks are ruptured mainly in an intergranular mode along their internal grain boundaries (Fig. S2). Considering the probabilistic nature for the failure of these ceramic bricks [26], a statistical analysis was performed to identify the dominant fatigue cracking features under both high and low $\Delta\sigma/2$. Such analysis indicated that the average number of ceramic bricks that were broken on the lateral surface within the range of 0.5 mm of the fracture plane was ~26 per square millimeter for relatively high $\Delta\sigma/2$, which was far less than that of 45 per square millimeter for the case of a relatively low $\Delta\sigma/2$. As such, the decrease in $\Delta\sigma/2$ results in a gradual transition in the mode of fa-

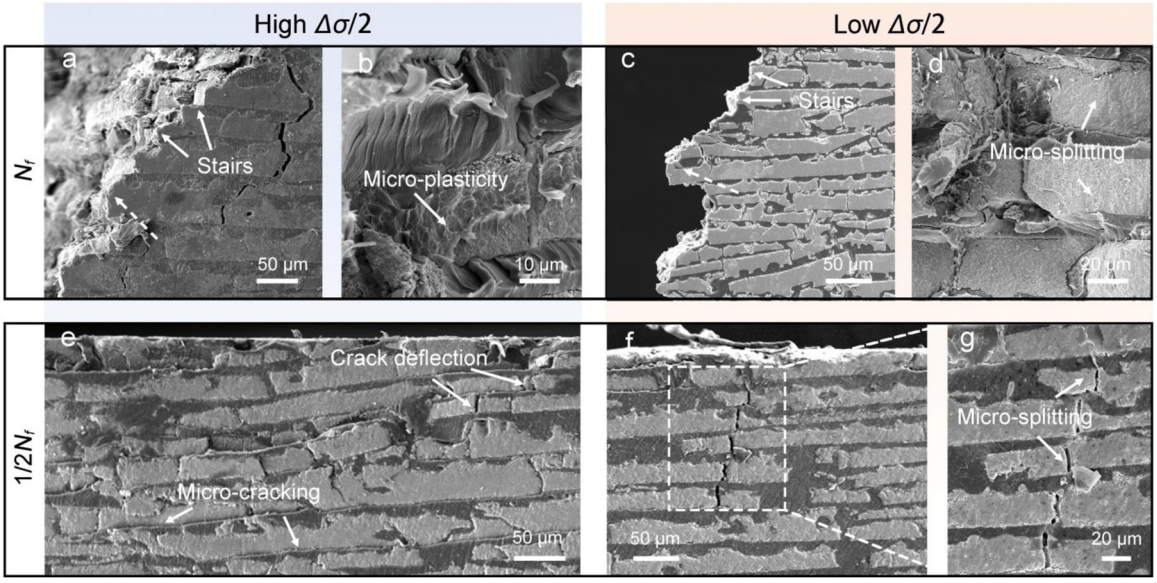

Fig. 2. Fatigue damage morphologies of the nacre-like composite. (a–d) SEM micrographs of the (a, c) lateral and (b, d) fracture surfaces of samples after loading to fracture under relatively (a, b) high and (c, d) low stress amplitudes $\Delta\sigma/2$, at 90 MPa and 65 MPa, respectively. (e–g) Surface damage morphologies of samples at half lifetime ($N_f/2$, without fracture) under relatively (e) high and (f, g) low $\Delta\sigma/2$. (g) is a magnified view of the dashed box in (f).

tigue cracking from separation along the inter-brick polymer phase to the fracture of the bricks in the composite.

Such a varying trend can be validated by examining the damage morphologies at half lifetimes, as shown in Fig. 2e–g. Under both high and low $\Delta\sigma/2$, the fatigue cracks tend to initiate near the contact surfaces of samples with the compression platens where stress concentrations are created. Nevertheless, microcracks are principally formed in the polymer phase in case of a high $\Delta\sigma/2$. The coalescence of these cracks between different layers is mainly realized by bypassing the bricks, leading to a zig-zag crack path with the formation of abundant "stairs" (Fig. 2e) [25]. In contrast, the bricks become more prone to splitting as $\Delta\sigma/2$ decreases. Fatigue cracking advances as the microcracks that form in the bricks at different layers propagate and connect by penetrating through the inter-layer polymer phase (Fig. 2f,g). As such, the width of the "stairs" is reduced, causing a decrease in the roughness of the crack surfaces.

In order to interpret the above effects of stress amplitude, a sample was cyclically loaded at a series of increasing stress amplitudes with the representative cyclic stress-strain curves shown in Fig. 3a. Hysteresis loops are formed because of the occurrence of internal friction in the composite [27]. This can clearly result from the polymer phase owing to its viscoelastic nature which is associated with the molecular rearrangement, *e.g.*, caused by the motion of side-groups on the molecular chains [28]. Nevertheless, other mechanisms, such as the repeated opening and closure of splitting cracks, the frictional sliding between mating crack surfaces, and the inelastic shearing of the polymer phase between ceramic bricks, may also act to promote the internal friction and dissipate mechanical energy [3,25,29]. In this regard, the strain energy release rate has been shown to play an important role in driving the growth of fatigue cracks [17,30]. As illustrated in Fig. 3b, for each loading-unloading cycle, the total input of mechanical energy by the loading process E_{total} can be divided into two parts: the elastic energy $E_{elastic}$ that can be restored during unloading and the dissipated energy $E_{dissipated}$ which is principally caused by internal friction and can be represented by the area of the hysteresis loop [31]. The internal friction can also be evaluated by the resultant inelastic strain amplitude $\Delta\varepsilon_{inelastic}$ which is the maximum distance between the loading and unloading curves at $\Delta\sigma/2$. As shown in Fig. 3c, both the proportion of dissipated energy in the total mechanical energy, $E_{dissipated}/E_{total}$, and $\Delta\varepsilon_{inelastic}$ display an increasing trend as $\Delta\sigma/2$ increases, indicating enhanced internal friction in the composite. In conjunction with the above damage morphologies, the reasons for such variations are deemed to be mainly twofold; specifically, the increase in $\Delta\sigma/2$ (i) promotes the intrinsic inelastic deformation of the polymer phase which helps to dissipate more mechanical energy, and (ii) favors a continuous deflection of the fatigue crack to increase the roughness or tortuosity of the crack trajectory, thereby facilitating the contact between splitting cracks and the frictional sliding between mating crack surfaces [17,32]. Both these mechanisms, respectively crack closure and crack surface interference, are potent mechanisms of crack-tip shielding which can serve to increase resistance to the growth of fatigue cracks [32].

Based on the above results, the fatigue cracking behavior and damage mechanisms in the nacre-like composite under cyclic compression are illustrated in Fig. 3d–f. The brick-and-mortar structure invariably plays a role in promoting the deflection of the fatigue crack along the interfaces between bricks, engendering the staircase-like fracture behavior (Fig. 3d) [25]. Nevertheless, the degree of this effect, in terms of the microscopic cracking characteristics, is closely associated with the applied stress amplitude. As shown in Fig. 3e,f, at relatively high $\Delta\sigma/2$, more prominent inelastic deformation occurs in the polymer phase. Cavities may then initiate at the deformed region, grow and coalesce under cyclic loads to develop into microcracks [33]. Fatigue cracks propagate primarily within the polymer phase between bricks; with such a mechanism, new microcracks constantly form ahead of the crack tip and connect to extend the crack. This acts to deflect the fatigue crack from the plane of maximum shear stress and leads to roughened fracture surfaces involving abundant micro "stairs" with a large fracture angle. As $\Delta\sigma/2$ decreases, the inelastic deformation in the polymer phase becomes less prominent; instead, fatigue damage mainly occurs in form of micro-splitting of the bricks by means of cracking along the internal grain boundaries within the bricks. The fatigue crack advances by connecting with the splitting cracks across the inter-layer polymer phase. As the microcracks between adjacent layers are not exactly in the same plane, micro "stairs" can still form on the fracture surfaces but are less evident. The

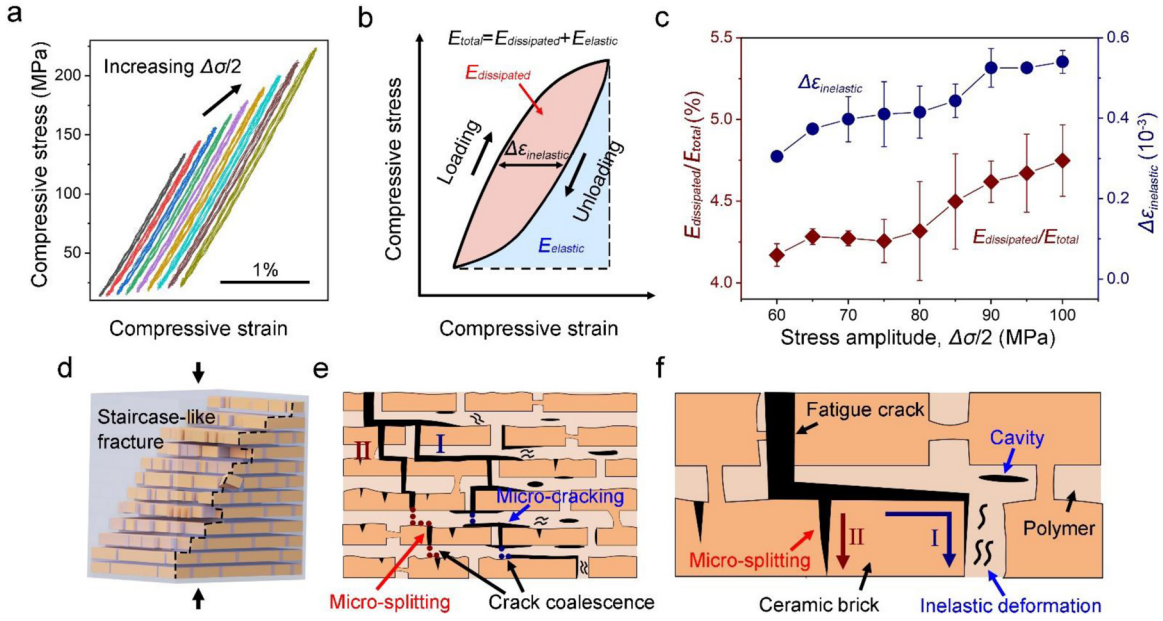

Fig. 3. Fatigue mechanisms of the nacre-like composite and the effects of stress amplitude. (a) Representative cyclic stress-strain curves of a composite sample under increasing stress amplitudes. (b) Illustration of an individual loading-unloading cycle and the characteristic parameters for analysis. (c) Variations in the proportion of dissipated mechanical energy in the total, $E_{dissipated}/E_{total}$, and the resultant inelastic strain amplitude, $\Delta\varepsilon_{inelastic}$, as a function of the applied stress amplitude $\Delta\sigma/2$. (d–f) Schematic illustrations of the fatigue fracture behavior and mechanisms in the nacre-like composite with brick-and-mortar structure under relatively (I) high and (II) low $\Delta\sigma/2$. The magnification increases from (d) to (f).

fracture angle also decreases toward the vertical direction where the splitting stress reaches the maximum (by contrast, the large fracture angle at high $\Delta\sigma/2$ favors a high shear stress which is beneficial for plastic deformation).

The maximum equivalent stress in human molars during clenching under a load of 200 N has been determined to be on the order of 66 MPa based on finite element simulations [22]. During mastication the maximum stress typically ranges from 24 MPa to 70 MPa depending on the elastic moduli of the food morsels. The fatigue endurance strength of the nacre-like composite, in terms of the stress amplitude (which at this stress ratio is actually about the mid-value of applied stress) is comparable to, or even higher than, the maximum stresses in human teeth (indeed, the maximum value of applied stress corresponding to such endurance strength is as high as ~150 MPa and far exceeds the stress level in human teeth) [22,23]. This implies a good potential of this composite for fulfilling the mechanical functions of dental applications.

The nacre-like brick-and-mortar structure may induce a series of mechanisms which are generally beneficial for resisting fatigue crack growth in materials. First, the deflection of fatigue crack along the polymer phase between bricks helps increase the overall length of crack path as compared to a straight cracking profile, and thereby prolongs the fatigue life to fracture [17,25]. The horizontal cracking between layers can also lead to ~90° deviation of the crack path from the vertical plane, thereby inhibiting the splitting fracture of composite. Similarly, the shear fracture can be made difficult by a constant crack deflection from the maximum shear stress plane by 45° along the zig-zag “stairs”. Second, the contact between mating crack surfaces during the fatigue cycle can be enhanced by the presence of abundant “stairs” [25]. This may disrupt the opening and closure of splitting cracks and also increase the resistance for shear fracture. Third, the final fracture of the composite necessitates the mutual sliding between neighboring bricks on the mating crack surfaces, which is particularly pertinent for the pull-out of bricks in the crack wake during fracture, as indicated by the dashed arrows in Fig. 2a. The sliding between bricks results in the inelastic deformation of the inter-brick polymer phase and dissipates more mechanical energy. It is noteworthy that the microcracking occurring either in the polymer phase at high $\Delta\sigma/2$ or in the bricks at low $\Delta\sigma/2$, where it plays an important role in deflecting the fatigue crack and increasing the roughness of crack surfaces. In addition, the tight bonding between the bricks and the polymer phase, which is realized by surface grafting of the ceramic scaffold before polymer infiltration, is critical for avoiding the easy interfacial cracking between the bricks, thereby ensuring the above effects of the brick-and-mortar structure.

In conclusion, a bioinspired nacre-like zirconia-PMMA composite has been shown to demonstrate a staircase-like fracture behavior under cyclic compression which results essentially from the deflection of fatigue crack induced by the brick-and-mortar structure. The extent of such an effect and the corresponding fatigue damage mechanisms are strongly dependent on the applied stress amplitude $\Delta\sigma/2$. An increase in $\Delta\sigma/2$ leads to a transition in the cracking mode from the fracture of bricks to separation along the inter-brick polymer phase. This is caused by increased internal friction as a result of the enhancement in the inelastic deformation of the polymer phase, the closure of splitting cracks and the frictional sliding between mating crack surfaces. The good fatigue properties, with the fatigue endurance strength being comparable to, or even exceeding, the maximum stress in human teeth during mastication, the human tooth-matching Young’s modulus and hardness, and the exceptional fracture toughness and machinability, endow this nacre-like composite with a good potential for dental applications. The clarification of its fatigue cracking behavior and damage mechanisms may also give insights for structural optimization toward enhanced fatigue resistance. Such a process may be effectively accelerated by the employment of data-driven approaches, *e.g.*, machine learning, which demonstrate a remarkable efficiency in large-scale explorations in materials science [34-36]. The combination of bioinspired designs with data-driven approaches may even facilitate the development of new fatigue-resistant materials.

Declaration of Competing Interest

The authors declare that they have no known competing financial interests or personal relationships that could have appeared to influence the work reported in this paper.

Acknowledgements

The authors are grateful for the financial support by the National Key R&D Program of China (2020YFA0710404), the KC Wong Education Foundation (GJTD-2020–09), the National Natural Science Foundation of China (51871216), the LiaoNing Revitalization Talents Program, and the Youth Innovation Promotion Association CAS. ROR acknowledges the support from the Multidisciplinary University Research Initiative to University of California Riverside, funded by the Air Force Office of Scientific Research (AFOSR-FA9550–15–1–0009) and subcontracted to the University of California Berkeley.

Supplementary materials

Supplementary material associated with this article can be found, in the online version, at doi:10.1016/j.scriptamat.2021.114089.

References

[1] M.A. Meyers, J. McKittrick, P.Y. Chen, Science 339 (2013) 773–779.
[2] E.M. Gerhard, W. Wang, C. Li, J. Guo, I.T. Ozbolat, K.M. Rahn, A.D. Armstrong, J. Xia, G. Qian, J. Yang, Acta Biomater. 54 (2017) 21–34.
[3] U.G.K. Wegst, H. Bai, E. Saiz, A.P. Tomsia, R.O. Ritchie, Nat. Mater. 14 (2015) 23–36.
[4] H.D. Espinosa, J.E. Rim, F. Barthelat, M.J. Buehler, Prog. Mater. Sci. 54 (2009) 1059–1100.
[5] D. Jiao, Z. Liu, Y. Zhu, Z. Weng, Z. Zhang, Mater. Sci. Eng. C 68 (2016) 9–17.
[6] R. Wang, Z. Suo, A. Evans, N. Yao, I.A. Aksay, J. Mater. Res. 16 (2001) 2485–2493.
[7] H. Gao, Y. Zhu, L. Mao, F. Wang, X. Luo, Y. Liu, Y. Lu, Z. Pan, J. Ge, W. Shen, Y. Zheng, L. Xu, L. Wang, W. Xu, H. Wu, S. Yu, Nat. Commun. 7 (2016) 1–8.
[8] E. Munch, M.E. Launey, D.H. Alsem, E. Saiz, A.P. Tomsia, R.O. Ritchie, Science 322 (2008) 1516–1520.
[9] F. Bouville, E. Maire, S. Meille, B. Van de Moortele, A.J. Stevenson, S. Deville, Nat. Mater. 13 (2014) 508–514.
[10] G. Tan, J. Zhang, L. Zheng, D. Jiao, Z. Liu, Z. Zhang, R.O. Ritchie, Adv. Mater. 31 (2019) 1904603.
[11] M. Grossman, F. Bouville, F. Erni, K. Masania, R. Libanori, A.R. Studart, Adv. Mater. 29 (2017) 1605039.
[12] Z. Hu, R. Guo, S. Chen, Q. Jin, P. Shen, Scr. Mater. 186 (2020) 312–316.
[13] N. Song, Y. Zhang, Z. Gao, X. Li, Nano Lett. 18 (2018) 5812–5820.
[14] L.J. Bonderer, A.R. Studart, L.J. Gauckler, Science 319 (2008) 1069–1073.
[15] C. Acevedo, V.A. Stadelmann, D.P. Pioletti, T. Alliston, R.O. Ritchie, Nat. Biomed. Eng. 2 (2018) 62–71.
[16] J.J. Kruzic, J.A. Arsecularatne, C.B. Tanaka, M.J. Hoffman, P.F. Cesar, J. Mech. Behav. Biomed. Mater. 88 (2018) 504–533.
[17] S. Suresh, Fatigue of Materials, 2nd Ed., Cambridge University Press, Cambridge, 1998.
[18] S. Wan, F. Xu, L. Jiang, Q. Cheng, Adv. Funct. Mater. 27 (2017) 1605636.
[19] J. Wang, Q. Cheng, L. Lin, L. Jiang, ACS Nano 8 (2014) 2739–2745.
[20] Y. Yang, B. Zhang, H. Wan, G. Zhang, J. Mater. Res. 33 (2018) 1543–1552.
[21] Z. Wang, M. Chen, Y. Liu, H. Duan, L. Xu, L. Zhou, J. Xu, J. Lei, Z. Li, J. Mater. Chem. C 7 (2019) 9018–9024.
[22] B. Dejak, A. Młotkowski, M. Romanowicz, J. Prosthet. Dent. 90 (2003) 591–597.
[23] I.M. Peterson, A. Pajares, B.R. Lawn, V.P. Thompson, E.D. Rekow, J. Dent. Res. 77 (1998) 589–602.
[24] G. Baran, K. Boberick, J. McCool, Crit. Rev. Oral Biol. Med. 12 (2001) 350–360.
[25] B. Gludovatz, M.D. Demetriou, M. Floyd, A. Hohenwarter, W.L. Johnson, R.O. Ritchie, Proc. Natl. Acad. Sci. USA 110 (2013) 18419–18424.
[26] W. Luo, Z.P. Bazant, Proc. Natl. Acad. Sci. USA 114 (2017) 12900–12905.
[27] J.E. Yagoubi, J. Lamon, J.C. Batsale, M.L. Flem, Acta Mater. 173 (2019) 302–312.
[28] J.D. Ferry, Viscoelastic Properties of Polymers, 3rd Ed., John Wiley & Sons, New York, 1980.
[29] H. Sehitoglu, Eng. Fract. Mech. 21 (1985) 329–339.
[30] S. Mall, G. Ramamurthy, M. Rezaizdeh, Compos. Struct. 8 (1987) 31–45.
[31] G. Fantozzi, P. Reynaud, Mater. Sci. Eng. A 521 (2009) 18–23.
[32] R.O. Ritchie, Mater. Sci. Eng. A 103 (1988) 15–28.
[33] N. Depoorter, D. Coutellier, M. Mužic, A. Berg-Pollack, Y. Cai, A. Zimmermann, Acta Mater. 54 (2006) 927–934.
[34] X. Liu, C.E. Athanasiou, N.P. Padture, B.W. Sheldon, H. Gao, Proc. Natl. Acad. Sci. USA 118 (2021) e2104765118.
[35] X. Liu, C.E. Athanasiou, N.P. Padture, B.W. Sheldon, H. Gao, Acta Mater. 190 (2020) 105–112.
[36] A.D. Spear, S.R. Kalidindi, B. Meredig, A. Kontsos, J.B. le Graverend, JOM 70 (2018) 1143–1146.